Electronic Supplementary Material (ESI) for Green Chemistry.

Supporting Information

Temperature-Induced Biphasic to Monophasic Transition as a Selectivity Switch in the Conversion of Xylose to Furfural

Luca Ricciardi,[a] Willem Verboom, *[,a] Jean-Paul Lange*[,b,c] and Jurriaan Huskens*[,a]

a. Molecular NanoFabrication group, Department of Molecules & Materials, MESA+ Institute for Nanotechnology , University of Twente, P.O. Box 217, 7500 AE, Enschede, The Netherlands.

b. Sustainable Process Technology group, University of Twente, P.O. Box 217, 7500 AE, Enschede, The Netherlands.

c. Shell Global Solutions Int. B.V. Grasweg 31, 1031 HW Amsterdam, The Netherlands.

Email and Tel:

(W.V.) w.verboom@utwente.nl, +31-53-489-2977.

(J.L.) j.p.lange@utwente.nl, +31-20-630-3428.

(J.H.) j.huskens@utwente.nl, +31-53-489-2995.

Table of Contents

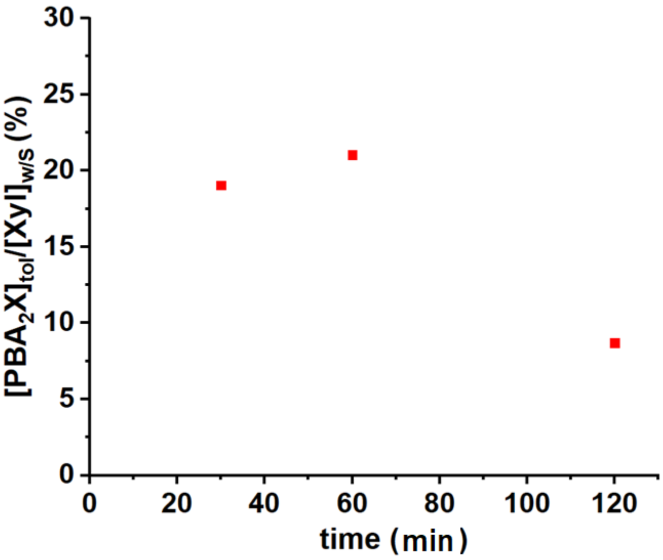

Figure S1. Ratio between the concentration of diester in the aromatic phase and the concentration of free xylose in the aqueous phase over time. These concentrations were evaluated by ^{1}H-NMR spectroscopy, at room temperature, and are used to calculate the overall xylose conversion. Specifically, total conversion (mol%) is evaluated based on the initial [PBA_2X] in the organic phase, taking in account the [PBA_2X] in the organic phase and the [Xylose] in the sulfolane-aqueous phase.

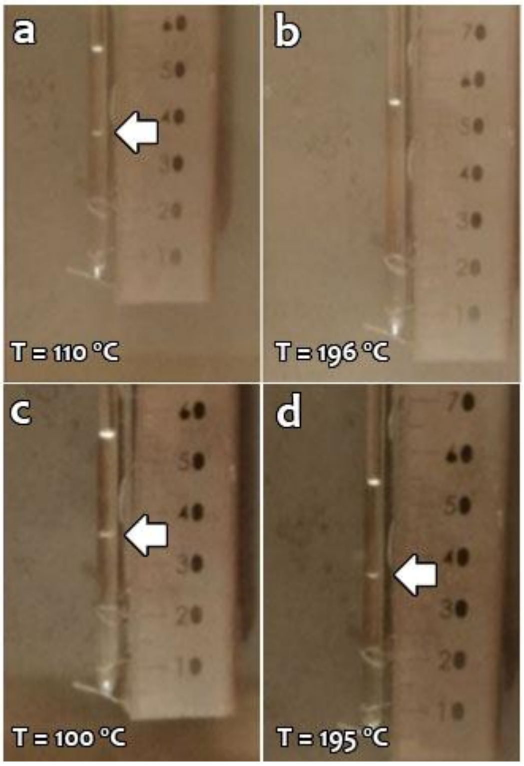

Figure S2. Comparison of solvent phase behavior in capillary tubes containing a 1:1:1 mixture of MN, sulfolane and water (pH = 1). On the top (a and b), the system contains 196 mM of PBA, and the meniscus, indicated by the arrow, disappears at high T (°C). On the bottom (c and d), the system contains no PBA, and the meniscus, indicated by the arrow, does not disappear at high T (°C).

Table S1. Xylose-to-furfural selectivities for a selection of points reported in Figure 4.

Temperature (°C)	[PBA] (mM)	Number of phases at reaction T (°C)	X-to-F selectivity mol%
150	3.3	2	63
150	667	2	65
150	67	2	67
200	2	2	67
150	17	2	71
180	2	2	73
165	667	1	89
205	10	1	91
180	100	1	95
180	197	1	96

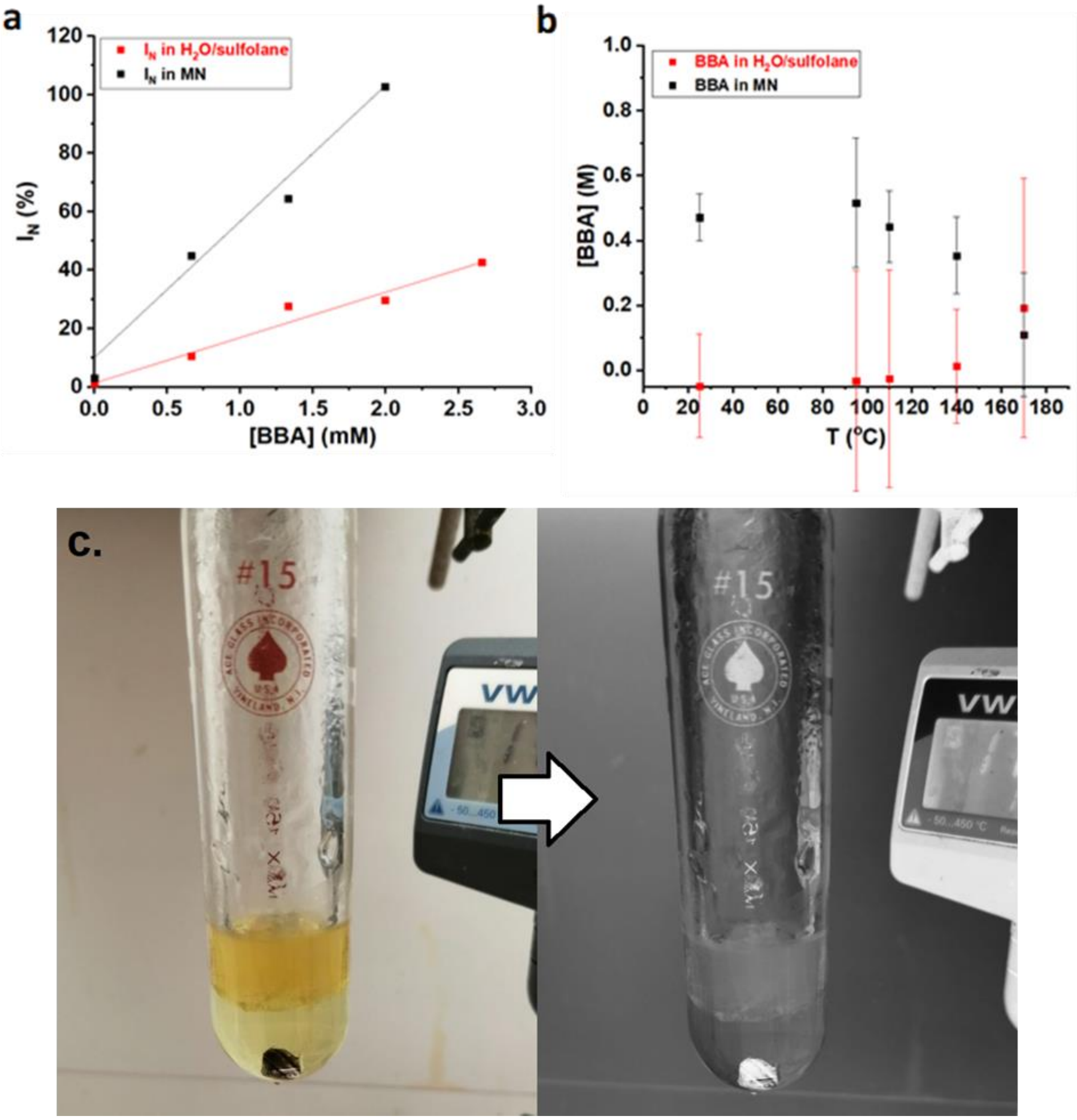

Figure S3. (a) Calibration curves to relate the concentration of 10-bromoanthracene-9-boronic acid (BBA) to the normalized color intensity, evaluated by analysing photographs of the solutions with ImageJ. (b) Relative concentrations, in MN and in water/sulfolane, of BBA with increasing temperature. (c) Characteristic photographs processing for the analysis.

Colorimetric study of the relative concentration of BBA – Data analysis

Each photograph was imported in ImageJ and the image type was changed from RGB to 8xbit, to eliminate the effect of the hue on the analysis. The picture was then inverted, to maximize the difference in intensity between signal and background (Figure S3c).

The relative intensity of the portion of the picture under analysis was evaluated using the function "histograms" of ImageJ. The standard error on the said intensity was evaluated dividing the standard deviation by the square root of the number of pixels of the selection, both of which are obtained as raw data from ImageJ.

The normalized intensity was calculated as a difference of the area in which we expect the signal and the background, both divided by the value of the background, to minimize the picture-to-picture fluctuations in luminosity and exposure (Equation S1).

$$I_N = 100 \cdot \left(\frac{I_{BBA}}{I_{BG}} - 1\right) \qquad \text{Equation S1}$$

In the calibration process, each of these values was coupled to a known concentration, and these relationships were used to obtain a linear fit, to allow evaluation of the concentrations in the cases under analysis.

The errors on each measurement were evaluated using standard error propagation theory.

Water Partial Pressure – Data analysis

A total volume of 75 mL of a 1:1:1 1-MN-sulfolane-water (pH =1) containing varying concentration of PBA has been heated from room temperature up to 190 °C in a 200 mL autoclave reactor.

Temperature and pressure of the system have been recorded in real time, the measurement was performed in triplicates for PBA concentrations in the whole mixture of 0, 23 and 117 mM. The raw data have been analysed, for each PBA concentration, in the following way:

1) The raw data for the 3 different runs at each concentration were grouped together in a P vs T array.
2) A temperature window of 0.5 °C was applied to the data set to divide the data in small groups (*e.g.*, all the data between 99.5 °C and 100.5 °C were grouped together and labeled "100 °C").
3) These data subgroups were averaged. The standard errors of the mean (SEM) of the subgroups were also evaluated.
4) As every T point is related to a P value, the same procedure was also applied point by point to the pressure dataset.

The result of this data analysis is a P vs T set of average datapoints (for each PBA concentration), for each T, with SEMs both on temperature and pressure. To evaluate the deviation from the "standard" behavior, the values at 0 mM of PBA were subtracted from the ones at 23 mM and 117 mM of PBA and plotted against T (°C).

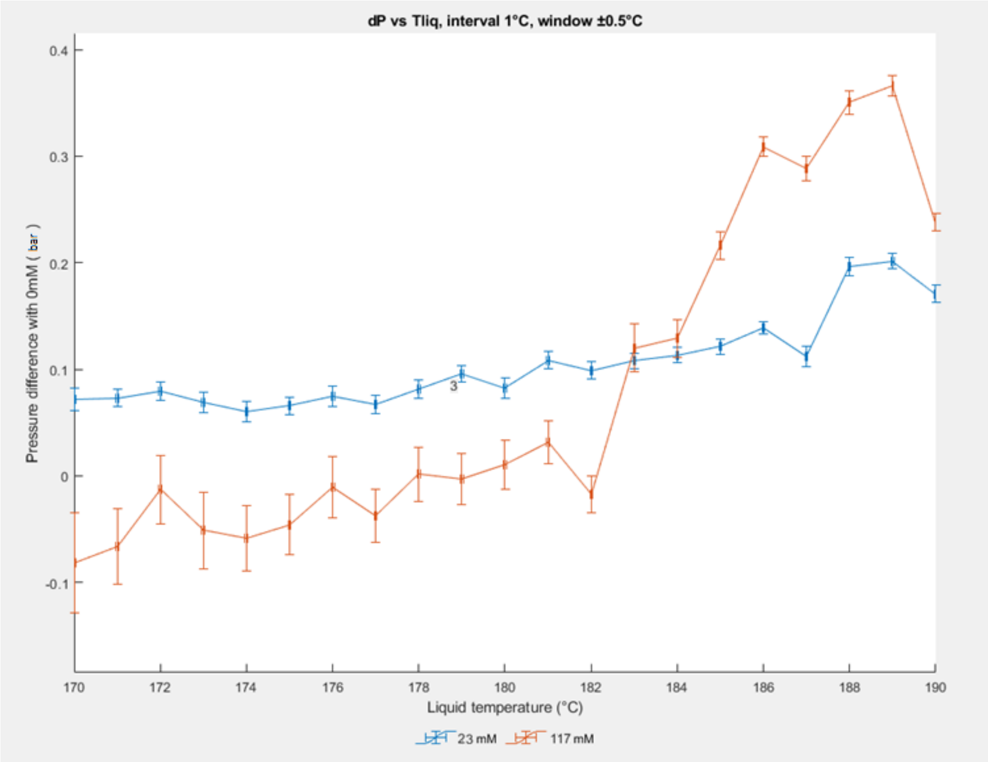

Figure S4. Difference in recorded pressure (dP) between the run with no PBA and the run with PBA at 23 mM (blue) and 117 mM (red) in the temperature range between 170 and 190 °C. The error bars on dP represent the standard error of the mean (SEM). Here we show the case in which the window was kept at 0.5 degrees.

Furthermore, the statistical significance of the deviation from the "standard" behavior was evaluated. For each dP the p-value was evaluated with the following procedure (all the formulas can be found in:

1) For each value of dP, the confidence interval (CI) was evaluated with a error margin of 95%

$$CI = \frac{(dP + \sigma_{dP}) - (\, dP - \sigma_{dP})}{2 \cdot 1.96}$$

2) Knowing the CI and the value of dP, the z-value was determined in its absolute value.

$$z = |\frac{dP}{CI}|$$

3) Using the z-value for each dP, the p-value was determined.

$$p = e^{(-0.717z + 0.416z^2)}$$

Table S2. Values of dP coupled with the SEM and the respective p-value.

	23 mM PBA			117 mM PBA		
	dP	σ_{dP}	p-value	dP	σ_{dP}	p-value
170	0.0718	0.0277	5,99E-07	-0.0816	0.0932	0,0858
171	0.0730	0.0262	7,97E-08	-0.0663	0.0721	0,0710
172	0.0793	0.0253	1,96E-09	-0.0128	0.0661	0,7171
173	0.0692	0.0283	2,26E-06	-0.0514	0.0741	0,1750
174	0.0604	0.0272	1,63E-05	-0.0588	0.0632	0,0678
175	0.0655	0.0247	3,00E-07	- 0.0461	0.0582	0,1209
176	0.0742	0.0258	3,14E-08	-0.0105	0.0592	0,7406
177	0.0666	0.0236	5,59E-08	-0.0374	0.0517	0,1571
178	0.0811	0.0243	1,56E-10	0.0014	0.0524	0,9617
179	0.0959	0.0241	4,20E-14	-0.0030	0.0513	0,9170
180	0.0824	0.0239	4,25E-11	0.0100	0.0476	0,6926
181	0.1086	0.0235	1,92E-18	0.0314	0.0434	0,1561
182	0.0989	0.0235	1,57E-15	-0.0172	0.0379	0,3789
183	0.1077	0.0214	2,04E-21	0.1199	0.0469	8,2052E-07
184	0.1133	0.0208	1,38E-24	0.1288	0.0379	8,2114E-11
185	0.1213	0.0202	1,72E-29	0.2161	0.0295	2,3216E-42
186	0.1390	0.0208	1,01E-35	0.3088	0.0254	1,355E-110
187	0.1118	0.0244	4,35E-18	0.2884	0.0271	8,5617E-86
188	0.1966	0.0227	5,63E-58	0.3503	0.0265	6,917E-130
189	0.2015	0.0214	7,54E-68	0.3658	0.0246	1,663E-163
190	0.1707	0.0255	6,63E-36	0.2378	0.0253	6,5834E-68

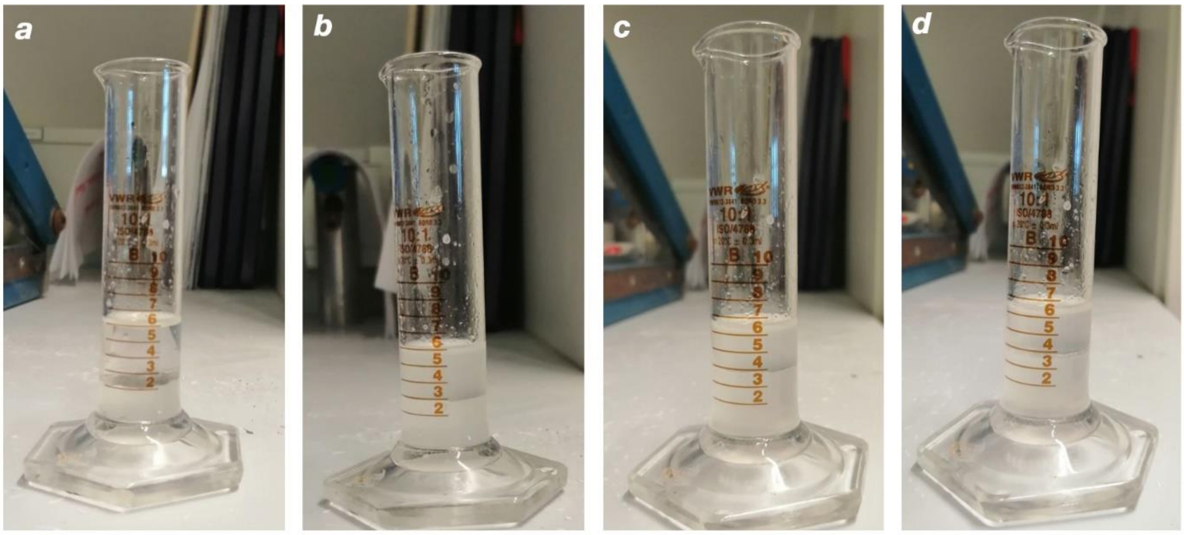

Figure S5. Comparison between the three-solvent system composed of equal volumes of water (pH = 1), toluene, and a third solvent, namely: (a) GVL, (b) dioxane, (c) DMSO and (d) sulfolane. Phase behavior and different partitioning of the polar organic solvents at room temperature. The water phase is always at the bottom and the toluene at the top, while the polar organic solvent is at the top (a), distributed over both (b), or at the bottom (c, d).

Table S3. Comparison between the three-solvent system composed of equal volumes of water (pH = 1), toluene and a polar organic solvent (listed in the table). Phase behavior at 180 ^{o}C at given PBA concentrations in toluene.

	0 mM	**590 mM**	**2000 mM**
Sulfolane	Biphasic	Monophasic	Monophasic
Dioxane	Biphasic	Biphasic	Biphasic
GVL	Biphasic	Biphasic	Biphasic

Table S4. Comparison of literature data about xylose dehydration performed in different solvent systems and the results obtained in this work using transient monophasic systems. Complete xylose conversion is reached in all cases. The column named “NoP” refers to the number of phases at the reaction temperature.

Solv. 1	Solv. 2	Solv. 3	NoP	Ratio	Catalyst	Sel. mol%	[Xyl] mM	T ^{o}C	Ref.
Water			1		H_2SO_4	45	350	200	2
DMSO			1		MCM-SO_3H	82	600	140	3
Water	Toluene		2	1:1	H_2SO_4	69	175	200	4
Water	DMSO		1	1:1	$SnCl_4$/LiCl	60	100	140	5
Water	1-Butanol		1	1:1	H_2SO_4	77	175	200	here
Water	DMSO		1	1:1	H_2SO_4	79	97	180	here
Water	Sulfolane		1	1:1	H_2SO_4	80	97	180	here
Water	Toluene	Sulfolane	1	1:1:1	H_2SO_4	95	97	180	here

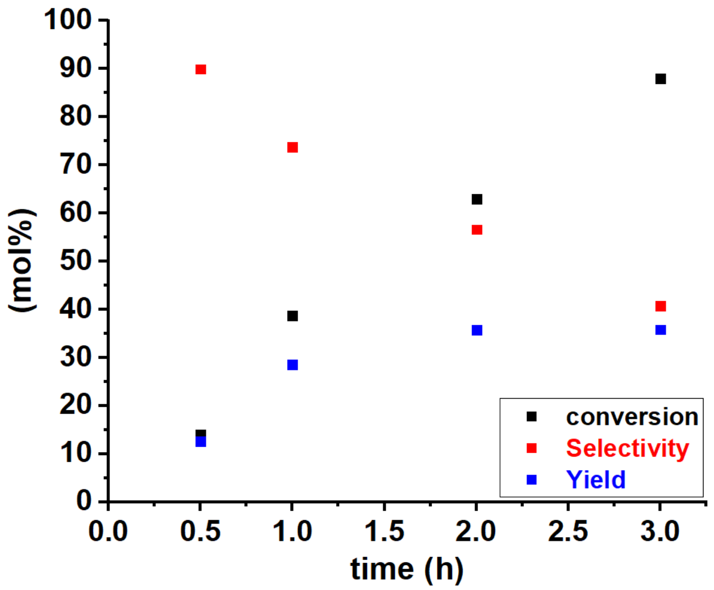

Figure S6. Relative concentrations (in mol% of the starting total free xylose concentration of 467 mM) of furfural and unconverted xylose, and the selectivity toward furfural vs time. Reaction performed in a 1:1:1 toluene-sulfolane-water (pH = 1) system at 180 °C with a concentration of PBA of 197 mM. Values calculated from NMR analysis of aqueous and toluene phases at r.t.

While the selectivity observed after 30 minutes is comparable with the system at low xylose concentration, in this case the selectivity does not stay constant but progressively lowers over time, reaching a maximum of approx. 30 mol% after 2 h of reaction. This maximum corresponds to a concentration of approx. 166 mM and 173 mM of furfural and unreacted xylose, respectively, in the system, which are values higher than when starting from a feed at 4-5 w% xylose concentration.

Table S5. Total concentration of furfural in the solvent system and ratio between the volumes of the polar and apolar phases. The presence of furfural > 130-140 mM influences the interaction between the solvents, affecting the relative volumes at r.t.

Xylose content (w%)	Time (h)	Total concentration of FUR in the system (mM)	V_{polar}/V_{apolar}
5	0,5	29	2
5	1	54	2
5	2	70	2
5	3	89	2
20	0,5	59	2
20	1	133	2
20	2	166	1
20	3	174	0.7

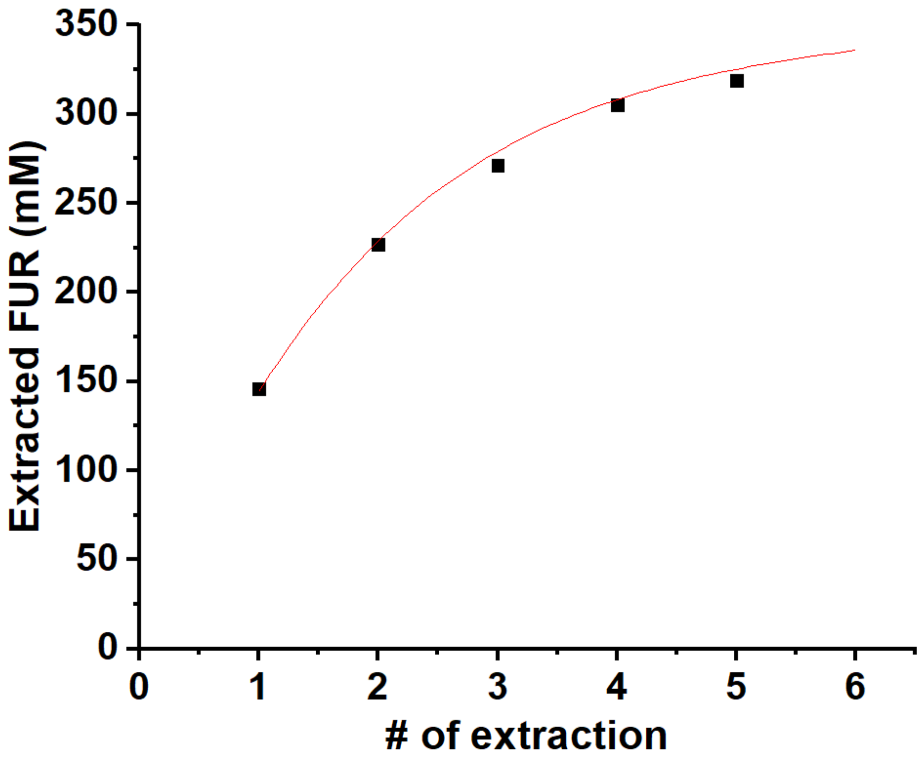

Figure S7. Furfural extraction with MN washings. (always 1:2 vol ratio between fresh toluene and residual S/W phase, performed at room temperature). The red line is calculated based on the theoretical partitioning shown in Table 2.

Alternative process concept

The xylose-extraction approach can be exploited for a 1-step process to produce furfural (Figure S6). Accordingly, the aqueous xylose hydrolysate is contacted with a solution of methylnaphthalene (MN)/phenylboronic acid (PBA)/sulfolane (S). The resulting stream is heated to the reaction temperature to convert the xylose and its boronate ester to furfural, then cooled to allow decantation into a apolar MN/PBA phase and a polar S/water phase. The apolar phase is distilled into a furfural top stream, the desired product stream, and MN/PBA bottom stream that is partly recycled to the dehydration reactor. The polar S/water stream is contacted with clean MN/BPA stream to recover the residual furfural and the resulting S/water stream is worked up to recover the sulfolane, for recycling to the dehydration reactor, and a residual hydrolysate effluent. This last work-up unit could consist e.g. of a membrane or an adsorption unit.

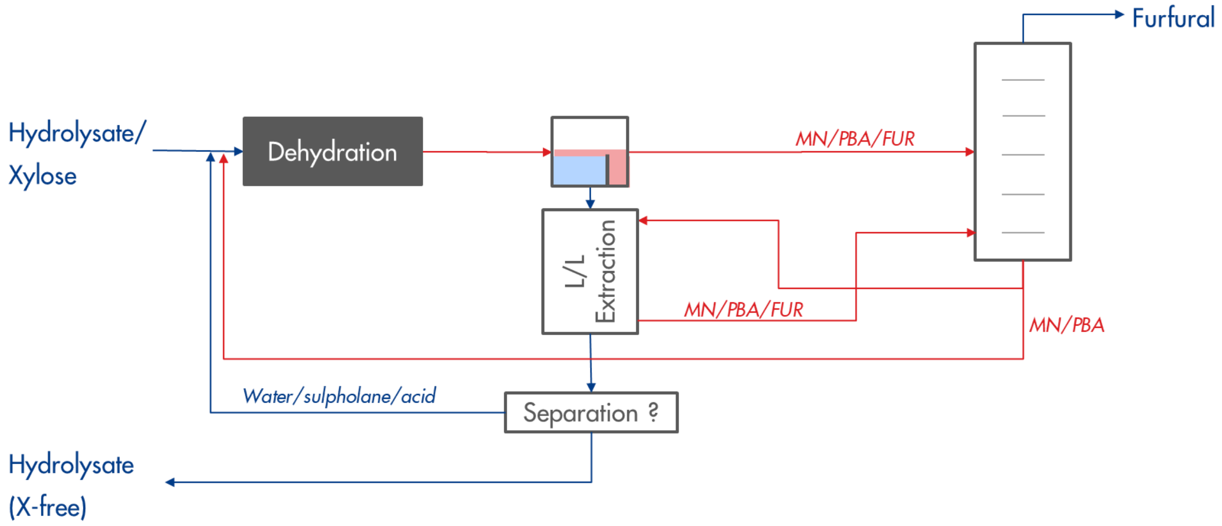

Figure S8. Conceptual process design for the 1-step furfural production.

The viability of such a scheme will depend on the possibility to properly close the recycle of S, MN and PBA. This implies that the final S-recovery unit is not leaving significant amounts of S, MN, BPA and furfural into the clean hydrolysate effluent. It also means that S, MN and PBA do not undergo significant chemical degradation during the process.

The furfural distillation is not expected to be challenging as illustrated by its low distillation resistance, defined by Lange *et al*.[6]

The process concept comprises three interlinked recycles that will need pilot for validation. We should indeed anticipate the build-up of undesired components in some of the recycle streams. Some could be by-products of the hydrolysis reaction, e.g. acetic acid. Others could be by-product of the dehydration reactions, e.g. humins as well as glucose degradation products. Proper management of such build-up will have to be considered in a later stage, once properly identified.

Preliminary economics

The process concept prosed here delivers a higher selectivity in furfural than the alternative concept based on dehydration in a single-phase aqueous medium or dehydration in bi-phasic water/organic media. However, the selectivity improvement is accompanied by an increase in process complexity to close the various recycles. We should then investigate whether the selectivity benefit is likely to pay for the increased process complexity.

Very preliminary, though insightful calculations have been developed to answer this question. They have been based on approach for preliminary economic screening proposed by Lange et al.,[6] and formulated as balancing the incomes and costs of the process according to the following equation.

*Product yield [t prod/t feed] * product price [$/t prod] > feed price [$/t feed] + conversion cost [$/t feed]*

First, the equation was used to estimate the price of xylose. We assumed here to pretreat biomass in a single step to produce a cellulosic pulp and aqueous xylose stream with 60 w% carbohydrate yield with a standard conversion cost of 200 $/t feed. We calculated a carbohydrate cost of 467 (±98)$/t, which we set to be equal for the pulp and the xylose by assuming that both would share the same outlet, e.g. fuel ethanol after hydrolysis of the cellulose/xylose mixture followed by co-fermentation. Such carbohydrate price is clearly higher than the ~300 $/t encountered for sugar syrup derived from starch or sugar crops. But this is consistent with the fact that cellulosic ethanol is more expensive than crop ethanol.

We then used this xylose price together with furfural market price of 1400 $/t and furfural yield of 70 and 95 mol%, i.e. 45 and 61 w% to estimate the maximal conversion cost that we can afford using the equation above. With 70 mol% xylose-to-furfural selectivity, the biphasic process is estimated to afford a conversion cost of 161 (±140) $/t, which falls within the range of a single process step. Hence, the biphasic process has reasonable chances of being affordable. Interestingly, however, the 95 mol% yield of the xylose extraction concept could afford a conversion cost of 385 (±162) $/t, i.e. could afford about two process steps instead of one. The overall conversion cost advantage amounts to 224 (±22) $/t, with a small uncertainty that results from the fact that the uncertainties of both scenarios are fully correlated; both need to use the same high/low xylose and furfural prices.

The premises used for these calculations are summarized below.

Table S6. Premises for preliminary economics

	unit	Value	Comment/source
Biomass price	$/t	80 (±20)	
Furfural price	$/t	1400 (±200)	
Conversion cost	$/t	200 (±50)	For a single process step
Carbohydrate yield	w% on biomass	60 (±5)	
Furfural yield	w% on xylose	45 (±3) or 61 (±3)	Based on yields of 70 and 95 mol%, resp.

Supporting videos:

Video S1. https://youtu.be/WM6hSonMHDE

Video S2. https://youtu.be/3bKxtz3u0Fg

References

1. J.-T. Lin, *Appl. Statist.*, **1989**, *38*, 69-70.
2. L. Ricciardi, W. Verboom, J.-P. Lange, J. Huskens, *ACS Sustain. Chem. Eng.* **2019**, *7*, 14273-14279.
3. A. S. Dias, M. Pillinger, A. A.Valente, *J. Catal.* **2005**, *229*, 414–423.
4. L. Ricciardi, W. Verboom, J.-P. Lange, J. Huskens, *ChemSusChem* **2020**, *13*, 3589-3593.
5. W. Wang, H. Li, J. Ren, R. Sun, J, Zheng, G. Sun, S. Liu, *Chinese J. Catal.* **2014**, *35*, 741–747.
6. J.-P. Lange, E. van der Heide, J. van Buijtenen, R. Price, *ChemSusChem* **2012**, *5*, 150-166.